Article

Extraction of Digital Cardiotocographic Signals from Digital Cardiotocographic Images: Robustness of eCTG Procedure

Agnese Sbrollini[ID], Lucia Brini, Maria Di Tillo, Ilaria Marcantoni[ID], Micaela Morettini and Laura Burattini *,†[ID]

Department of Information Engineering, Università Politecnica delle Marche, 60121 Ancona, Italy; a.sbrollini@pm.univpm.it (A.S.); brinilucia@gmail.com (L.B.); ditillomaria@gmail.com (M.D.T.); i.marcantoni@pm.univpm.it (I.M.); m.morettini@univpm.it (M.M.)

*   Correspondence: l.burattini@univpm.it; Tel.: +39-071-220-4461
†   For research purposes, eCTG can be obtained for free by contacting the corresponding author (Laura Burattini, l.burattini@univpm.it).

check for updates

Abstract: A recently developed software application, eCTG, extracts cardiotocographic (CTG) signals from digital CTG images, possibly obtained by scanning paper CTG reports. The aim of this study was to evaluate eCTG robustness across varying image formats, resolution and screw. Using 552 digital CTG signals from the "CTU-UHB Intrapartum Cardiotocography Database" of Physionet, seven sets of digital CTG images were created, differing in format (.TIFF, .PNG and .JPEG), resolution (96 dpi, 300 dpi and 600 dpi) and screw (0.0°, 0.5°, and 1.0°). All created images were submitted to eCTG for CTG signals extraction. Quality of extracted signals was statistically evaluated based 1) on signal morphology, by computation of the correlation coefficient (ρ) and of the mean signal error percent (MSE%), and 2) on signal clinical content, by assessment of 18 standard CTG variables. For all sets of images, ρ was high ($\rho \geq 0.81$) and MSE% was small (MSE% $\leq 2\%$). However, significant changes occurred in median values of four, four and five standard CTG variables in image sets with 96 dpi resolution, 0.5° screw and 1.0° screw, respectively. In conclusion, for an optimal eCTG performance, digital images should be saved in lossless formats, have a resolution of at least 300 dpi and not be affected by screw.

Keywords: cardiotocography; fetal monitoring; computerized cardiotocography; biomedical signal processing; biomedical image processing; electronic clinical applications

1. Introduction

Despite availability of other tests [1–3], cardiotocography (CTG) remains the most popular clinical evaluation for fetal well-being assessment worldwide [4,5]. Clinicians typically interpret the two simultaneously acquired CTG signals, namely fetal heart rate (FHR, bpm) and maternal uterine contraction (UC, mmHg) by visual inspection. Consequently, diagnosis is subjective and strongly dependent on the clinician's experience, so that CTG sensitivity and specificity are still far from being satisfying [6]. Computerized CTG analysis [7,8] has been proposed to contrast inter-subject variability of visual CTG interpretation and to increase CTG reliability. Still, the lack of databases of digital CTG signals have limited the spread of automatic CTG analysis procedures, due to testing difficulties.

For a long time CTG reports have been printed on paper for clinical consultation, a practice that is still very common nowadays. As a consequence, maternal hospitals have stored databases of paper CTG reports that take up a lot of space, are difficult to manage, are subject to deterioration over time and are not used in retrospective CTG studies to promote computerized CTG analysis [8].

Recently, a software procedure termed eCTG was proposed as a tool to extract FHR and UC signals from digital CTG images [9], possibly including those obtained by scanning paper CTG reports. Thus, eCTG represents a suitable tool to transform paper CTG databases into digital CTG databases, which are much easier to store, maintain and manage, and more useful for research studies. The scanning process is quite simple, but the quality of the resulting image is dependent on scanner settings (image format type and resolution) [10] and on user/scanner ability to avoid the screw effect (image orientation in relation to the scanner). Clearly, quality of extracted FHR and UC signals depends on the quality of the scanned CTG image. The previous study on eCTG provided the description of an algorithm to extract FHR and UC signals from CTG images saved in .TIFF format, with a resolution of 300 dpi and without screw. The aim of this study was to evaluate eCTG robustness with varying image format, resolution and screw.

2. Materials and Methods

2.1. Data

All digital CTG images used in this study were created starting from CTG signals (from now on called original signals) recorded in 552 pregnant women (singleton pregnancies and gestational age > 36 weeks) during labor (duration of stage 2 of labor was at most 30 minutes) using external ultrasound probes. Original signals were at most 90 min long and sampled at 4 Hz. All acquisitions occurred at the Czech Technical University and the University Hospital in Brno and are available at the "CTU–UHB Intrapartum Cardiotocography Database" [11] by Physionet [12]. All Physionet data are fully anonymized and may be used without further Institutional Review Board approval.

Digital CTG images were created (Figure 1) using MATLAB by plotting the above-mentioned original signals on a proper CTG grid in order to reproduce CTG reports [9]. Then, images were saved by selecting format, resolution and screw. Specifically, considered formats were .TIFF, .PNG and .JPEG; the considered resolutions used were 96 dpi, 300 dpi and 600 dpi; eventual screw levels, described by image rotation angles, were 0.0°, 0.5°, and 1.0°. Overall, 7 sets of data (S1 to S7) were created, each containing 552 digital CTG images homogeneous for format, resolution and screw, as reported in Table 1. Sets S2 to S7 were obtained by varying only one feature with respect to S1. Indeed, S1 (.TIFF, 300 dpi, no screw) was previously used as eCTG validation set in [9], and thus was taken as reference. Sets S2 and S3 served to test eCTG robustness to varying format, S4 and S5 to varying resolution and S6 to S7 to varying screw.

2.2. The eCTG Software Application

All created images were submitted to the eCTG software application to extract original signals. The block diagram of the eCTG algorithm is depicted in Figure 2. Briefly, the input in an eCTG procedure is the digital CTG image. The first step of eCTG is the screw correction: initially, the algorithm analyses the digital CTG image to detect the CTG grid corners; then it computes the screw angle (α) between the horizontal line (matching the upper edge of the digital CTG image) and the line connecting the upper CTG grid corners; and finally, it corrects the screw effect by rotating the digital CTG image by $-\alpha$. Then, eCTG splits the input digital CTG image (in RGB, obtained by scanning a paper CTG report or electronically created as done here) into two sub-images (in RGB), namely FHR image and UC image, and independently (but analogously) processes them to extract the signals of interest, the digital FHR signal and the digital UC signal, respectively. At first, each sub-image undergoes preprocessing during which it is converted from RGB to grayscale and properly resized so that the sampling frequency of the successively extracted signal will be 4 Hz. Then, the preprocessed sub-image undergoes thresholding to be converted into a black-and-white mask in which the background is black and the signal is white. Finally, the signal is extracted by recognition of white pixels and calibrated in amplitude.
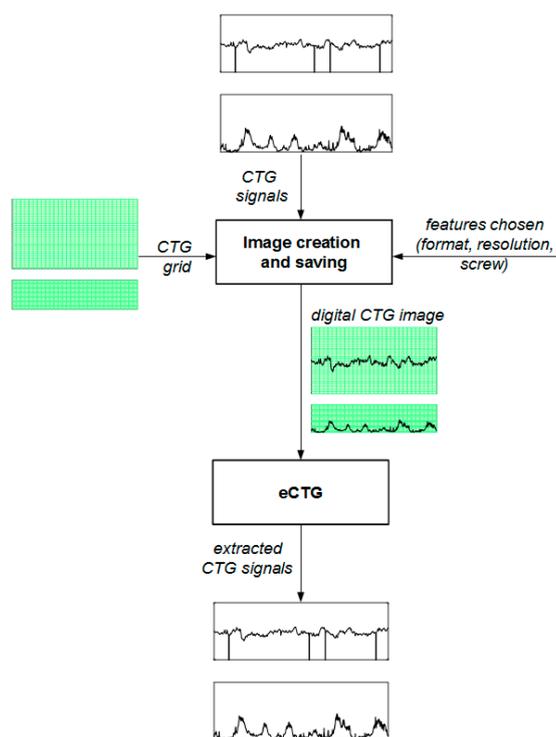
Figure 1. Creation of digital cardiotocographic (CTG) images and extraction of CTG signals. Original CTG signals from the 'CTU-UHB Intrapartum Cardiotocography Database' are plotted on a CTG grid and saved according to features (format, resolution and screw) chosen by the user. The obtained digital CTG images are submitted to eCTG in order to get the extracted CTG signals.

Table 1. Features (format, resolution and screw) associated to each set of images.

	S1	S2	S3	S4	S5	S6	S7
Format	.TIFF	.PNG	.JPEG	.TIFF	.TIFF	.TIFF	.TIFF
Resolution (dpi)	300	300	300	96	600	300	300
Screw (°)	0	0	0	0	0	0.5	1

2.3. Statistical Signal Quality Evaluation

Quality of extracted FHR and UC signals was statistically evaluated based on signal morphology and signal clinical content. Statistical evaluation based on signal morphology consisted of the computation of the Pearson's correlation coefficient (ρ) and of the mean signal error percent (MSE%, computed as the mean amplitude difference between the original signal and the extracted signal, normalized according to the amplitude of the original signal) between CTG signals extracted from a digital image and the corresponding original ones. Statistical evaluation based on signal clinical content required assessment of a set of clinical variables from each signal, which was performed using CTG Analyzer [8], an application for automatic analysis of CTG signals. Specifically, CTG Analyzer receives as input the CTG signals and processes them to provide the following 18 standard clinical CTG variables: FHR baseline (BL, bpm); FHR baseline variability (BLV, bpm); number, mean amplitude and mean duration of tachycardia episodes (#TC; ATC, bpm; DTC, min); bradycardia episodes (#BC; ABC, bpm; DBC, min); acceleration episodes (#AC; AAC, bpm; DAC, min) and deceleration episodes (#DC; ADC, bpm; DDC, min); number, mean amplitude, mean duration and period of uterine contractions (#UC; AUC, mmHg; DUC, s; PUC, min).
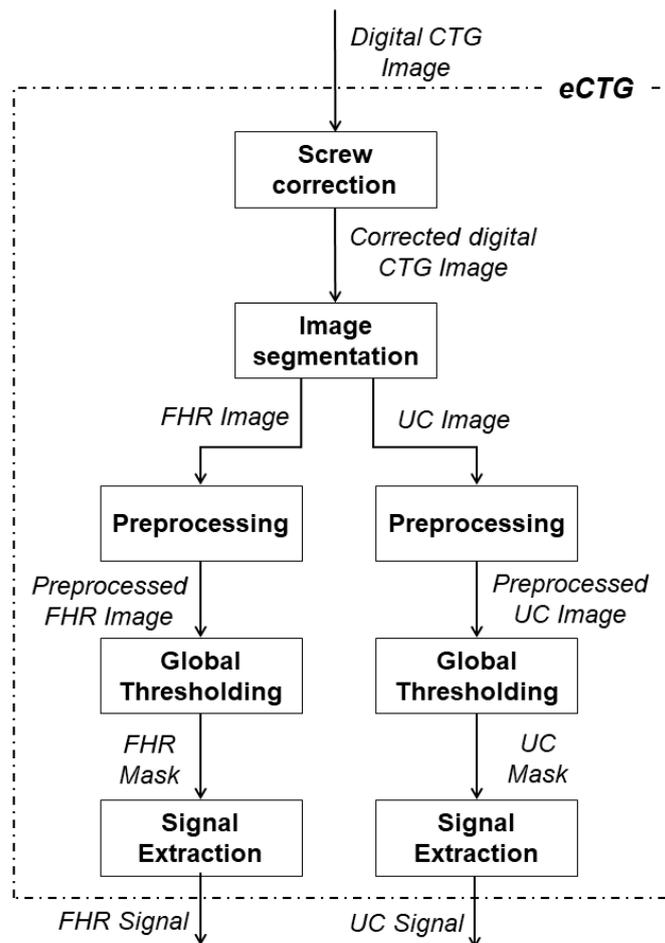
Figure 2. Block diagram of eCTG algorithm used to extract digital fetal heart rate (FHR) and uterine contraction (UC) signals from digital CTG images.

Normality of distributions of ρ, MSE% and clinical variables within each set of images was evaluated using the Lilliefors test, with the null hypothesis being a non-normal distribution. The nonparametric Wilcoxon rank sum test was used to compare median feature values of non-normal distributions, which were described in terms of 50th[25th; 75th] percentiles. Statistical significance level (P) was set at 0.05 in all cases.

3. Results

Results of the statistical evaluation of signal quality based on signal morphology are reported in Table 2. For all sets of images, ρ values (all statistically significant) were high (ρ ≥ 0.81 for FHR and ρ ≥ 0.92 for UC) and MSE% values were small (MSE% ≤ 2% for FHR and MSE% ≤ 2% for UC). The image sets showing the best results were S1 (FHR: ρ = 0.85, MSE% = 1%; UC: ρ = 0.97, MSE% = 0%) and S5 (FHR: ρ = 0.85, MSE% = 1%; UC: ρ = 0.97, MSE% = 0%); the image sets showing the worst results were S4 (FHR: ρ = 0.81, MSE% = 2%; UC: ρ = 0.92, MSE% = 1%), S6 (FHR: ρ = 0.86, MSE% = 1%; UC: ρ = 0.93, MSE% = 2%) and S7 (FHR: ρ = 0.85, MSE% = 1%; UC: ρ = 0.94, MSE% = 2%). Only median values of MSE% distributions for UC signals over S6 ($P < 10^{-168}$) and S7 ($P < 10^{-164}$) significantly differed from median value of MSE% distribution over S1 (Table 2).

Results of the statistical evaluation of signal quality based on signal clinical content are reported in Table 3. Sets of images with median clinical variables differing the most from original signals were: S4, with four variables statistically different, namely BLV ($P < 10^{-5}$), AAC ($P < 0.05$), DAC ($P < 10^{-4}$) and DDC ($P < 10^{-6}$); S6, with four variables statistically different, namely BL ($P < 0.05$), BLV ($P <$

0.01), ADC (P < 10^{-7}), and AUC (P < 0.01); and S7 with five variables statistically different, namely BL (P < 0.05), BLV (P < 0.01), ADC (P < 10^{-7}), DDC (P < 0.01) and AUC (P < 0.01).

4. Discussion

The aim of this paper was to evaluate eCTG robustness to varying format, resolution and screw associated with digital CTG images from which CTG signals could be extracted. To this end, seven sets of digital CTG images were created; each set contained 552 images and was characterized by a specific combination of three possible formats (.TIFF, .PNG and .JPEG), three resolution values (96 dpi, 300 dpi and 600 dpi) and three screw angles (0.0°, 0.5°, 1.0°). Among the three considered formats, two were lossless, namely .TIFF and .PNG, and one was lossy, namely .JPEG. The three resolution values represent the standard ones for low-resolution (96 dpi), medium-resolution (300 dpi), and high-resolution (600 dpi) images. The three screw angles simulate the typical, not-easily-visible, manually-induced interference occurring during paper scanning. In order to perform a robustness evaluation of our algorithm, it was essential to understand which feature is more critical in terms of CTG signal quality. Thus, we decided to vary only one feature in each set of images.

Quality of FHR and UC signals extracted from created digital CTG images was statistically evaluated based on signal morphology and on signal clinical content, differently from other algorithms present in literature [13]. For clinical evaluations, 18 standard CTG variables for fetal health assessment according to the most popular CTG interpretation guidelines [14–17] were considered.

For example, high BLV and high #AC, AAC and DAC indicate fetal well-being, while low BLV and high #DC, ADC and DDC are associated with fetal distress [18,19].

In relation to eCTG robustness to format, with a resolution of 300 dpi and no screw, no significant differences were observed between results obtained with .TIFF and .PNG, while BLV obtained using .JPEG was significantly lower (P < 0.05) than that obtained using .TIFF (Table 3). Consequently, when using eCTG, lossless formats for CTG images should be preferred. In relation to eCTG robustness to resolution, with .TIFF format and no screw, no significant differences were observed between results obtained with 600 dpi vs. 300 dpi, while robustness of four clinical variables was significantly reduced when using a 96 dpi resolution (Table 3). Consequently, when using eCTG, low-resolution CTG images should not be used and a resolution of at least 300 dpi is required.

Table 2. Results of statistical evaluation of signal quality based on signal morphology. Distribution of ρ and MSE% are reported in terms of 50th[25th;75th] percentiles.

		S1	S2	S3	S4	S5	S6	S7
FHR	ρ	0.85 [0.77;0.9]	0.85 [0.76;0.9]	0.85 [0.76;0.9]	0.81 [0.69;0.9]	0.85 [0.76;93]	0.86 [0.78;0.9]	0.85 [0.78;0.9]
	MSE%	1 [1;2]	1 [0;2]	1 [0;2]	2 [1;3]	1 [0;2]	1 [1;2]	1 [1;2]
UC	ρ	0.97 [0.95;0.9]	0.93 [0.87;0.9]	0.96 [0.93;0.9]	0.92 [0.86;0.9]	0.97 [0.94;0.9]	0.93 [0.89;0.9]	0.94 [0.89;0.9]
	MSE%	0 [0;0]	1 [0;1]	0 [0;0]	1 [0;1]	0 [0;0]	2 ** [1;3]	2 ** [1;3]

*,**, P-value lower than 0.05 and 0.01, respectively, when comparing signal morphology variables computed from S2–S7 against those computed from S1.

Table 3. Clinical variables distribution of all CTG signals extracted by eCTG. Non-normal distributions are reported in terms of 50th[25th;75th] percentiles.

	Original Signals	S1	S2	S3	S4	S5	S6	S7
BL **(bpm)**	132 [123;141]	132 [123;141]	131 [122;140]	132 [122;140]	131 [122;140]	132 [123;141]	134 * [126;141]	134 * [126;141]
BLV **(bpm)**	16 [12;20]	16 [12;19]	16 [12;19]	15 * [12;19]	15 ** [11;18]	16 [12;19]	15 ** [11;19]	15 ** [11;19]
#TC	0 [0;0]	0 [0;0]	0 [0;0]	0 [0;0]	0 [0;0]	0 [0;0]	0 [0;0]	0 [0;0]
ATC **(bpm)**	0 [0;0]	0 [0;0]	0 [0;0]	0 [0;0]	0 [0;0]	0 [0;0]	0 [0;0]	0 [0;0]
DTC **(min)**	0 [0;0]	0 [0;0]	0 [0;0]	0 [0;0]	0 [0;0]	0 [0;0]	0 [0;0]	0 [0;0]
#BC	0 [0;1]	0 [0;1]	0 [0;1]	0 [0;1]	0 [0;1]	0 [0;1]	0 [0;1]	0 [0;1]
ABC **(bpm)**	0 [0;77]	0 [0;79]	0 [0;79]	0 [0;78]	0 [0;81]	0 [0;79]	0 [0;94]	0 [0;93]
DBC **(min)**	0 [0;10]	0 [0;10]	0 [0;10]	0 [0;10]	0 [0;10]	0 [0;10]	0 [0;10]	0 [0;10]
#AC	5 [3;9]	6 [3;9]	5 [3;9]	5 [3;9]	6 [3;9]	5 [3;9]	5 [3;9]	5 [3;9]
AAC **(bpm)**	149 [141;158]	148 [141;157]	148 [140;157]	148 [140;158]	147 * [139;156]	148 [141;158]	149 [140;157]	148 [140;157]
DAC **(min)**	1 [1;2]	1 [1;2]	1 [1;2]	1 [1;2]	1 ** [1;2]	1 [1;2]	1 [1;2]	1 [1;2]
#DC	6 [3;10]	6 [3;10]	6 [3;10]	6 [3;10]	6 [3;10]	6 [3;10]	6 [3;10]	6 [3;10]
ADC **(bpm)**	102 [93;110]	102 [93;111]	102 [93;111]	101 [93;111]	101 [93;111]	102 [93;111]	106 ** [97;113]	106 ** [97;113]
DDC **(min)**	1 [1;1]	1 [1;1]	1 [1;1]	1 [1;1]	1 ** [1;1]	1 [1;1]	1 [1;1]	1 ** [0;1]
#UC	18 [12;23]	17 [12;23]	18 [12;23]	18 [12;23]	17 [11;23]	18 [13;23]	17 [12;23]	17 [12;23]
AUC **(mmHg)**	35 [28;45]	35 [28;45]	35 [28;44]	35 [28;45]	35 [28;44]	35 [28;45]	33 ** [26;42]	33 ** [26;42]
DUC **(min)**	1 [1;2]	1 [1;2]	1 [1;2]	1 [1;2]	1 [1;2]	1 [1;2]	1 [1;2]	1 [1;2]
PUC **(min)**	4 [3;4]	4 [3;4]	4 [3;4]	4 [3;4]	4 [3;4]	4 [3;4]	4 [3;4]	4 [3;4]

*,**, P-value lower than 0.05 and 0.01, respectively, when comparing clinical variables computed from extracted signals against those computed from original signals.

The screw is the most problematic issue in digital signal extraction from scanned digital images. The application of the original version of eCTG [9] on S6 and S7 sets provided the worst results in terms of signal morphology (FHR: $\rho = 0.85$, MSE% = 1%; UC: $\rho = 0.95$, MSE% = 2%, for S6; FHR: $\rho = 0.84$, MSE% = 2%; UC: $\rho = 0.90$, MSE% = 5% for S7) and of signal clinical content (S6, with median values of seven variables statistically different, namely BLV, #BC, ABC, ADC, DDC, #UC and AUC; and S7 with median values of nine variables statistically different, namely BLV, #BC, ABC, DBC, #AC, ADC, DDC, AUC and DUC). Thus, in this paper an updated version of eCTG was presented, including

a preprocessing procedure for screw correction. With .TIFF format and 300 dpi resolution, four and five clinical variables were significantly different when compared with results obtained with 0.5° and 1.0° screw, respectively, against those obtained with no screw (Table 3). Despite the good results provided by the screw correction algorithm, we recommended always paying attention while scanning, in order to prevent images being affected by the screw effect. Considering the high level of distortion introduced by screw (even when corrected), automatic scanning should be preferred over manual scanning, since this is less likely to introduce the screw effect.

5. Conclusions

For an optimal extraction of FHR and UC signals by eCTG, digital CTG images should be saved in lossless formats, have a resolution of at least 300 dpi and not be affected by screw.

Author Contributions: Conceptualization, methodology and software, A.S. and M.D.T.; validation, investigation and data curation, L.B. (Lucia Brini); writing—original draft preparation, A.S. and L.B. (Laura Burattini); writing—review and editing, L.B. (Lucia Brini), I.M. and M.M.; supervision, L.B. (Laura Burattini).

References

1. Agostinelli, A.; Marcantoni, I.; Moretti, E.; Sbrollini, A.; Fioretti, S.; Di Nardo, F.; Burattini, L. Noninvasive Fetal Electrocardiography Part I: Pan-Tompkins' Algorithm Adaptation to Fetal R-peak Identification. *Open Biomed. Eng. J.* **2017**, *11*, 17–24. [CrossRef] [PubMed]

2. Agostinelli, A.; Sbrollini, A.; Burattini, L.; Fioretti, S.; Di Nardo, F.; Burattini, L. Noninvasive Fetal Electrocardiography Part II: Segmented-Beat Modulation Method for Signal Denoising. *Open Biomed. Eng. J.* **2017**, *11*, 25–35. [CrossRef] [PubMed]

3. Sbrollini, A.; Strazza, A.; Caragiuli, M.; Mozzoni, C.; Tomassini, S.; Agostinelli, A.; Morettini, M.; Fioretti, S.; Di Nardo, F.; Burattini, L. Fetal Phonocardiogram Denoising by Wavelet Transformation: Robustness to Noise. In Proceedings of the 2017 Computing in Cardiology (CinC), Rennes, France, 24–27 September 2017; pp. 1–4.

4. Alfirevic, Z.; Gyte, G.M.L.; Cuthbert, A.; Devane, D. Continuous cardiotocography (CTG) as a form of electronic fetal monitoring (EFM) for fetal assessment during labour. *Cochrane Database Syst. Rev.* **2017**, *2*, CD006066. [CrossRef] [PubMed]

5. Ayres-De-Campos, D.; Nogueira-Reis, Z.; Information, P.E.K.F.C. Technical characteristics of current cardiotocographic monitors. *Best Pr. Res. Clin. Obstet. Gynaecol.* **2016**, *30*, 22–32. [CrossRef] [PubMed]

6. Todros, T.; Preve, C.; Plazzotta, C.; Biolcati, M.; Lombardo, P. Fetal heart rate tracings: Observers versus computer assessment. *Eur. J. Obstet. Gynecol. Reprod. Boil.* **1996**, *68*, 83–86. [CrossRef]

7. Ovhed, I.; Johansson, E.; Odeberg, H.; Råstam, L. A Comparison of Two Different Team Models for Treatment of Diabetes Mellitus in Primary Care. *Scand. J. Caring Sci.* **2000**, *14*, 253–258. [CrossRef] [PubMed]

8. Sbrollini, A.; Agostinelli, A.; Burattini, L.; Morettini, M.; Di Nardo, F.; Fioretti, S.; Burattini, L. CTG Analyzer: A graphical user interface for cardiotocography. In Proceedings of the 2017 39th Annual International Conference of the IEEE Engineering in Medicine and Biology Society (EMBC), Seogwipo, South Korea, 11–15 July 2017; pp. 2606–2609.

9. Sbrollini, A.; Agostinelli, A.; Marcantoni, I.; Morettini, M.; Burattini, L.; Di Nardo, F.; Fioretti, S.; Burattini, L. eCTG: An automatic procedure to extract digital cardiotocographic signals from digital images. *Comput. Methods Programs Biomed.* **2018**, *156*, 133–139. [CrossRef] [PubMed]

10. Gonzalez, R.; Woods, R. Digital image processing and computer vision. *Comput. Vision, Graph. Image Process.* **1990**, *49*, 122.

11. Chudáček, V.; Spilka, J.; Burša, M.; Janků, P.; Hruban, L.; Huptych, M.; Lhotská, L. Open access intrapartum CTG database. *BMC Pregnancy Childbirth* **2014**, *14*, 16. [CrossRef] [PubMed]

12. Goldberger, A.L.; Amaral, L.A.N.; Glass, L.; Hausdorff, J.M.; Ivanov, P.C.; Mark, R.G.; Mietus, J.E.; Moody, G.B.; Peng, C.C.-K.C.-K.; Stanley, H.E. PhysioBank, PhysioToolkit, and PhysioNet: Components of a New Research Resource for Complex Physiologic Signals. *Circulation* **2000**, *101*, e215–e220. [CrossRef] [PubMed]

13. Cömert, Z.; Şengür, A.; Akbulut, Y.; Budak, Ü.; Kocamaz, A.F.; Bajaj, V. Efficient approach for digitization of the cardiotocography signals. *Phys. A Stat. Mech. its Appl.* **2020**, *537*, 122725. [CrossRef]

14. Ayres-De-Campos, D.; Spong, C.Y.; Chandraharan, E.; Panel, F.I.F.M.E.C. FIGO consensus guidelines on intrapartum fetal monitoring: Cardiotocography. *Int. J. Gynecol. Obstet.* **2015**, *131*, 13–24. [CrossRef] [PubMed]

15. Shields, L.E.; Goffman, D.; Caughey, A. ACOG practice bulletin: Clinical management guidelines for obstetrician-gynecologists. *Obstet. Gynecol.* **2017**, *130*, e168–e186.

16. National Collaborating Centre for Women's and Children's Health (UK). *Intrapartum Care: Care of Healthy Women and Their Babies During Childbirth.* BMJ (Online) Published online 03 December 2014. Available online: www.bmj.com/content/349/bmj.g6886 (accessed on 1 September 2019).

17. Zhao, Z.; Zhang, Y.; Deng, Y. A Comprehensive Feature Analysis of the Fetal Heart Rate Signal for the Intelligent Assessment of Fetal State. *J. Clin. Med.* **2018**, *7*, 223. [CrossRef] [PubMed]

18. Sbrollini, A.; Carnicelli, A.; Massacci, A.; Tomaiuolo, L.; Zara, T.; Marcantoni, I.; Burattini, L.; Morettini, M.; Fioretti, S.; Burattini, L. Automatic Identification and Classification of Fetal Heart-Rate Decelerations from Cardiotocographic Recordings. In Proceedings of the 2018 40th Annual International Conference of the IEEE Engineering in Medicine and Biology Society (EMBC), Honolulu, HI, USA, 18–21 July 2018; pp. 474–477.

19. Agostinelli, A.; Palmieri, F.; Biagini, A.; Sbrollini, A.; Burattini, L.; Di Nardo, F.; Fioretti, S.; Burattini, L. Relationship between Deceleration Areas in the Second Stage of Labor and Neonatal Acidemia. In Proceedings of the 2016 Computing in Cardiology Conference (CinC), Vancouver, BC, Canada, 11–14 September 2016.